

# Crystalline Silicon Heterojunction Solar Cells With Metal Oxide Window Layers

Erenn Ore<sup>1</sup>, Gehan Amaratunga<sup>1</sup>

<sup>1</sup>Department Of Engineering, University Of Cambridge, Cambridge, United Kingdom.

**Abstract** — For the crystalline silicon (c-Si) heterojunction (HJ) solar cell with the conventional structure, the parasitic absorbance in the window contact layer (WCL) of p-type doped thin film silicon or its alloy (pDTF-Si/A) limits the amount of the short circuit current density ( $J_{sc}$ ) generated. In this work, pDTF-Si/A is replaced with a transition metal oxide (TMO) of  $MoO_x$ ,  $WO_x$ ,  $TiO_x$ ,  $NiO_x$ ,  $Cu_2O_x$ . Due to the wide band gaps of TMO materials, the c-Si HJ cells with TMO WCLs have higher  $J_{sc}$  than the conventional c-Si HJ cell under AM1.5 irradiation. The values of the excess charge carrier lifetime and the implied open circuit voltage indicate that  $WO_x$  provides the best passivation for c-Si.

**Index Terms** — heterojunction, silicon, solar cell, transition metal oxide.

## I. INTRODUCTION

A conventional solar cell core structure consists of a photon absorbing layer called the absorber (A), and two wider band gap contact layers on either side of the absorber. The contact layer, through which impinging photons enter the absorber first, is referred to as the window contact layer (WCL). The other contact layer is referred to as the back contact layer (BCL). The core photovoltaic element of an absorber layer sandwiched between a WCL and a BCL is abbreviated as WAB, after the initial letter of each layer of the core element. A basic solar cell structure is completed by contacting WAB with a different electrode on either side. Typically, WCL is contacted with a transparent front electrode (TFE), and BCL is contacted with a reflective back electrode (RBE). Photons enter the solar cell from the TFE side. Therefore, in order to achieve high short circuit current density ( $J_{sc}$ ), it is critical to employ a TFE | WCL pair with good photon transmission capability.

When crystalline silicon (c-Si) wafer is used as the absorber, the resulting WAB solar cell is referred to as the c-Si WAB solar cell, Figure 1, where all of the other layers are deposited onto the wafer.

Since recombination at the c-Si surface is high due to the high density of non-saturated bonds [1], a key requirement for achieving high power conversion efficiency for the c-Si WAB solar cell is to employ a WCL and BCL pair that is able to passivate the c-Si wafer surfaces well, reducing the charge carrier recombination at the wafer surfaces to a negligible level.

In a conventional heterojunction c-Si WAB solar cell design, WCL is made up of a layer of intrinsic hydrogenated amorphous silicon (i - a-Si:H) and a layer of boron doped (p-type) thin film silicon or its alloy (pDTF-Si/A), which is

typically p-type hydrogenated amorphous silicon (p - a-Si:H); and BCL is made up of a layer of i - a-Si:H and a layer of phosphorus doped (n-type) thin film silicon or its alloy, which is typically n-type hydrogenated amorphous silicon (n - a-Si:H). Thus, in this conventional heterojunction c-Si WAB solar cell design, i - a-Si:H covers both faces of the wafer. The i - a-Si:H buffer layers provide the required interface passivation [2][3] between the c-Si wafer and the layers of doped thin film silicon or its alloy, which provide the charge carrier selectivity [3]. In the literature, this conventional c-Si WAB solar cell design is referred to as the c-Si heterojunction solar cell with intrinsic thin layer, i.e. the HIT cell [3].

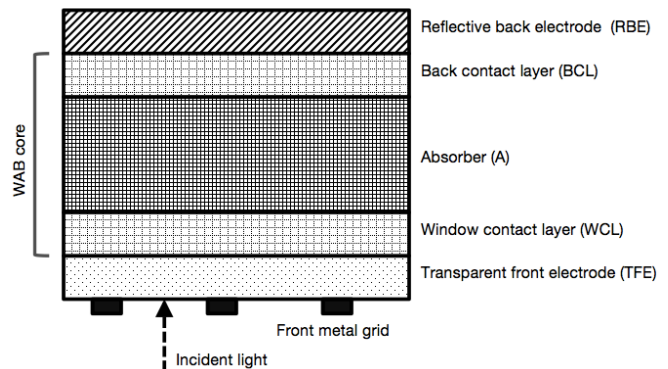


Fig. 1. A schematic representation of a WAB solar cell structure with the c-Si wafer absorber, which also functions as the substrate.

For the c-Si WAB solar cells, including the HIT cell, one of the main challenges for improving the power conversion efficiency has been the pDTF-Si/A based WCL [4]. Because of the high density of tail states in its band gap, the pDTF-Si/A layer absorbs a significant portion of the incoming light [5][6]. However, the charge carriers generated by light absorption in the pDTF-Si/A layer do not contribute to  $J_{sc}$  of the cell, because of the high recombination rates in pDTF-Si/A [7]. In addition, pDTF-Si/A is typically processed by chemical vapour deposition (CVD) from diborane, which contains the boron dopant. Diborane is known to be associated with significant health and safety related concerns [8]. Hence, handling diborane requires strict safety regulations and also the use of elaborate containment systems [9]. These requirements inevitably increase the processing costs and complexity of c-Si WAB solar cells.

In the c-Si WAB cell design investigated here, pDTF-Si/A is replaced by one of the transition metal oxides (TMO) of

$\text{MoO}_x$ ,  $\text{WO}_x$ ,  $\text{TiO}_x$ ,  $\text{NiO}_x$ , and  $\text{Cu}_2\text{O}_x$ . In our previous investigation, this concept is successfully demonstrated with TMO of non-stoichiometric vanadium pentoxide ( $\text{V}_2\text{O}_x$ ) [10]. Furthermore, this concept was also demonstrated for thin film WAB solar cells [11]-[13].

Due to their wider band gaps with respect to the band gap of pDTF-Si/A, the use of aforementioned TMOs would be expected to increase the amount of incoming light reaching the absorber, especially over the visible spectrum, consequently increasing the amount of  $J_{\text{SC}}$  generated by the cell. Another advantage of these TMOs is that they can be deposited at low-temperatures by simple physical vapour deposition (PVD) methods, including thermal evaporation. This would reduce the processing complexity and cost of the c-Si WAB solar cell.

## II. CELL STRUCTURE AND PROCESSING

For the c-Si WAB solar cells processed in this investigation, a textured, phosphorous doped c-Si (n - c-Si) wafer is used as the substrate, which also functions as the absorber, Figure 2.

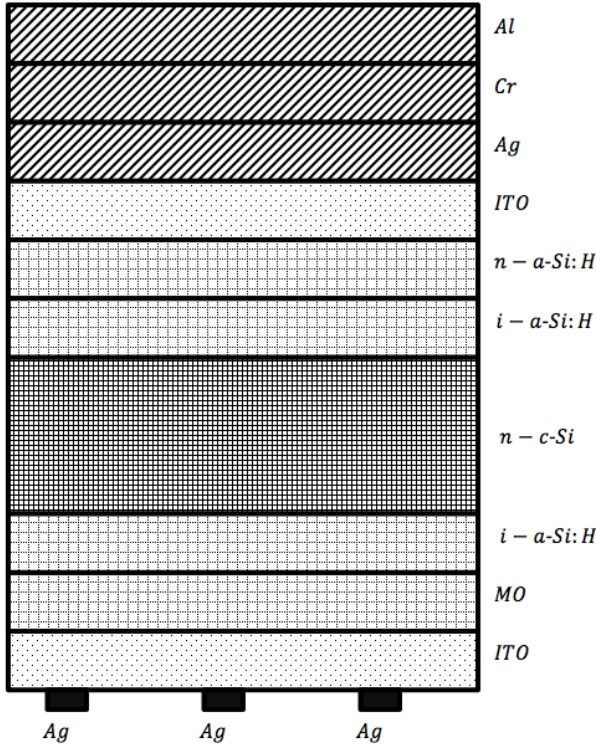


Fig. 2. A schematic representation of the c-Si WAB cell, where the p - a-Si: H layer is replaced by a metal oxide (MO) window layer.

All solar cells investigated here have an indium tin oxide (ITO) TFE, a RBE with the structure of ITO, silver, chromium, and aluminium (ITO | Ag | Cr | Al), and a BCL made up of an n - a-Si: H layer and an i - a-Si: H buffer layer. WCL is made up of an i - a-Si: H buffer layer, and a layer of either p - a-Si: H or TMO. The cell with the p - a-Si: H layer is referred to as the reference cell. The fully processed c-Si WAB solar cells have the common structure of ITO (100 nm) |

p - a-Si: H or TMO | i - a-Si: H (6 nm) | n - c-Si wafer | i - a-Si: H (6 nm) | n - a-Si: H (20 nm) | ITO (150 nm) | Ag (300 nm) | Cr (50 nm) | Al (400 nm). The 100 nm thick ITO TFE is also covered by a silver grid, Figure 2. All TMOs are deposited by thermal evaporation at room temperature.

## III. CELL CHARACTERISATION

A WCT 120 photoconductance lifetime tester system (Sinton Instruments) is used for the excess charge carrier concentration ( $\delta n$ ) measurements, which are carried out on the solar cell precursors prior to ITO deposition. The lifetime ( $\tau$ ) values of the excess charge carriers, and the implied open circuit voltage ( $V_{\text{OC|imp}}$ ) values are stated at  $\delta n = 10^{15} \text{ cm}^{-3}$ .

A suns- $V_{\text{OC}}$  illumination voltage tester system (Sinton Instruments) is used for measuring the quasi-steady-state open circuit voltage ( $Q_{\text{ss}}V_{\text{OC}}$ ) of the cells. From these data, current density versus voltage (JV) curves are constructed by using the superposition principle. The pseudo-fill factor ( $\text{FF}_{\text{PSE}}$ ) is then determined from the associated JV curve [14]. Note that,  $\text{FF}_{\text{PSE}}$  excludes the effect of series resistance [14][15], hence it gives the highest possible value for the fill factor.

The  $J_{\text{SC}}$  values are determined from the external quantum efficiency ( $\eta_{\text{EQ}}$ ) measurements by using an in-house built  $\eta_{\text{EQ}}$  measurement system with a solar simulator of 1 sun intensity, corresponding to the AM1.5 irradiation, operating at room temperature under the short circuit condition.

## IV. RESULTS AND DISCUSSION

Compared to the reference cell, the higher  $\eta_{\text{EQ}}$  values of the c-Si WAB cells with TMOs, Figure 3, indicate that  $\text{MoO}_x$ ,  $\text{WO}_x$ ,  $\text{TiO}_x$ , and  $\text{NiO}_x$  are more effective than p - a-Si: H in letting the high energy photons, i.e. photons with shorter wavelengths, enter the absorber. This would explain the high  $J_{\text{SC}}$  values for the c-Si WAB cells with TMOs, Table 1.

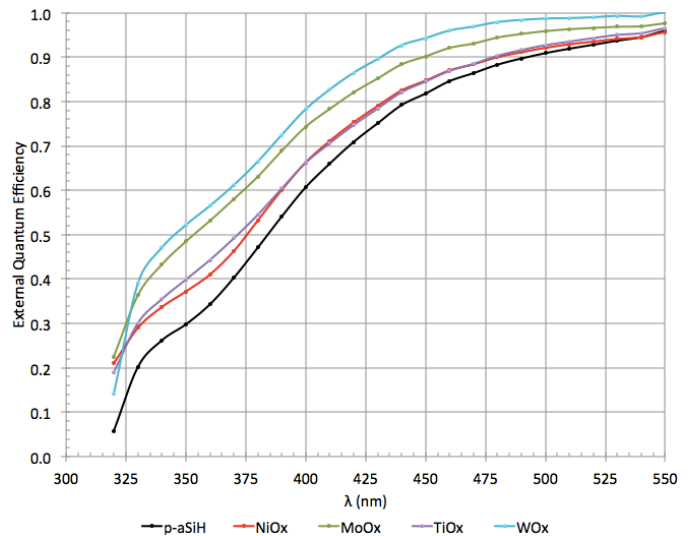


Fig. 3. The external quantum efficiency data for the c-Si WAB cells with different WCLs for  $320 \text{ nm} \leq \lambda \leq 550 \text{ nm}$ , where  $\lambda$  is the wavelength of the impinging photons.

TABLE 1. THE  $J_{SC}$  VALUES FOR THE c-Si WAB CELLS WITH THE TMO BASED WCLS, AS CALCULATED FROM THE  $\eta_{EQ}$  MEASUREMENT DATA. ‡: EACH WCL INVESTIGATED HERE ALSO HAS A 6 NM THICK i – a-Si: H LAYER. †: THE  $J_{SC}$  VALUE FOR THE c-Si WAB CELL WITH THE  $Cu_2O_x$  BASED WCL IS FROM THE JV MEASUREMENT (UNDER THE AM1.5 IRRADIATION AT ROOM TEMPERATURE), WHICH UNDERESTIMATES THE VALUE OF  $J_{SC}$ . THIS IS PRIMARILY DUE TO THE IMPERFECT MATCH BETWEEN THE ACTIVE CELL AREA DEFINED BY THE SHADOW MASK DURING CELL DEPOSITION AND MASKING OF THE AREA SURROUNDING IT BY A PIECE OF ANTI-REFLECTIVE COATING DURING JV MEASUREMENTS, AND ALSO DUE TO THE SHADOWING EFFECTS OF THE JV MEASUREMENT PROBES.

WCL‡	$J_{SC}$ (mA/cm <sup>2</sup> )
WO <sub>x</sub>	40.82
TiO <sub>x</sub>	39.83
NiO <sub>x</sub>	39.15
MoO <sub>x</sub>	39.43
Cu <sub>2</sub> O <sub>x</sub>	37.02†

Since reducing the interface defect density is critical for achieving high power conversion efficiency, what needs to be determined first is whether TMO, together with i – a-Si: H, can passivate c-Si wafer surface well. One way of investigating this is to look into the  $\tau$  data for the solar cell precursors prior to ITO deposition. The  $\tau$  data and the associated estimated values of  $V_{OC|imp}$  and of the reverse saturation current density ( $J_{S1}$ ) are given in Table 2.

TABLE 2. THE  $\tau$ ,  $V_{OC|imp}$ , AND  $J_{S1}$  VALUES FOR THE PRECURSORS OF THE c-Si WAB CELLS WITH DIFFERENT TMO BASED WCLS, PRIOR TO ITO DEPOSITION. ‡: EACH WCL INVESTIGATED HERE ALSO HAS A 6 NM THICK i – a-Si: H LAYER.

WCL‡	$\tau$ (ms)	$V_{OC imp}$ (mV)	$J_{S1}$ (A/cm <sup>2</sup> )
WO <sub>x</sub>	2.458	729	$3.12 \times 10^{-15}$
TiO <sub>x</sub>	2.421	722	$1.17 \times 10^{-14}$
MoO <sub>x</sub>	0.735	698	$2.22 \times 10^{-14}$
Cu <sub>2</sub> O <sub>x</sub>	0.790	707	$7.63 \times 10^{-14}$
NiO <sub>x</sub>	0.113	623	$6.79 \times 10^{-13}$
p – a-Si: H	2.205	722	$5.63 \times 10^{-15}$

The  $\tau$  data indicate that all of the aforementioned TMO based WCLS, except the NiO<sub>x</sub> based WCL, provide good c-Si surface passivation. In particular, the cells with the WO<sub>x</sub> based WCL and with the TiO<sub>x</sub> based WCL have the  $\tau$  values of 2.458 ms and 2.421 ms respectively, which are higher than  $\tau = 2.205$  ms measured for the reference cell. This implies that the WO<sub>x</sub> based WCL and the TiO<sub>x</sub> based WCL provide better surface passivation for c-Si than the p – a-Si: H based WCL.

$J_{S1}$  is a good indicator for the effectiveness of WCL, since, for a given photocurrent, reducing  $J_{S1}$  is correlated with

increasing the open circuit voltage. The c-Si WAB cell with WO<sub>x</sub> based WCL has the lowest  $J_{S1}$  at  $3.12 \times 10^{-15}$  A/cm<sup>2</sup>. Therefore, this cell has the highest  $V_{OC|imp}$ , which is a benchmark for the largest possible value for the open circuit voltage.

Since the c-Si WAB solar cell with the WO<sub>x</sub> based WCL has both the highest  $\tau$  value and the lowest  $J_{S1}$  value, it can be concluded that the WO<sub>x</sub> based WCL provides better c-Si surface passivation, compared to the p – a-Si: H based WCL, and to the other TMO based WCLS investigated here.

The  $FF_{PSE}$  values determined from the  $Q_{SS}V_{OC}$  measurement data for the reference c-Si WAB cell with the p – a-Si: H based WCL and for the c-Si WAB cell with the WO<sub>x</sub> based WCL are given in Table 3.

TABLE 3. THE  $FF_{PSE}$  VALUES FROM THE  $Q_{SS}V_{OC}$  DATA FOR THE REFERENCE c-Si WAB CELL WITH THE p – a-Si: H BASED WCL AND FOR THE c-Si WAB CELL WITH THE WO<sub>x</sub> BASED WCL. ‡: EACH WCL INVESTIGATED HERE ALSO HAS A 6 NM THICK i – a-Si: H LAYER.

WCL‡	$FF_{PSE}$
WO <sub>x</sub>	0.880
p – a-Si: H	0.811

## V. CONCLUSION

$J_{SC}$  of 40.82 mA/cm<sup>2</sup>,  $V_{OC|imp}$  of 0.729 V and  $FF_{PSE}$  of 0.880 measured for the c-Si WAB cell with the WO<sub>x</sub> based WCL imply that this cell has the potential to achieve a higher power conversion efficacy than the conventional c-Si WAB solar cells with the pDTF-Si/A based WCLS.

An additional benefit of using WO<sub>x</sub> instead of pDTF-Si/A is that WO<sub>x</sub> is deposited by a simple, low temperature thermal evaporation method, which eliminates the use of dangerous diborane gas from the c-Si WAB solar cell manufacturing process. Therefore, in addition to improving the power conversion efficiency, using a WO<sub>x</sub> based WCL has the potential to make the c-Si WAB solar cell manufacturing process safer, simpler and cheaper.

We thank the management team of the Photovoltaics Laboratory of Microengineering Institute, Ecole Polytechnique Fédérale de Lausanne, Neuchâtel, Switzerland for giving us access to the Photovoltaics Laboratory for this work.

## REFERENCES

- [1] A. G. Aberle, "Surface passivation of crystalline silicon solar cells: a review," *Progress In Photovoltaics: Research And Applications*, vol. 8, pp. 362-376, 2000.
- [2] J. I. Pankove, M. L. Tarnag, "Amorphous silicon as a passivant for crystalline silicon," *Applied Physics Letters*, vol. 34, issue 2, pp. 156-157, 1979.
- [3] W. G. J. H. M. van Sark, L. K. F. Roca, *Physics and Technology of Amorphous-Crystalline Heterostructure Silicon Solar Cells*. Berlin & Heidelberg, Germany: Springer-Verlag, 2012.

- [4] Z. C. Holman, A. Descoedres, L. Barraud, F. Z. Fernandez, J. P. Seif, S. De Wolf, C. Ballif, "Current losses at the front of silicon heterojunction solar cells," *IEEE Journal of Photovoltaics*, vol. 2, issue 1, pp. 7-15, 2012.
- [5] M. R. Page, E. Iwaniczko, Y. Q. Xu, L. Roybal, F. Hasoon, Q. Wang, R. S. Crandall, "Amorphous / crystalline silicon heterojunction solar cells with varying i-layer thickness," *Thin Solid Films*, vol. 519, issue 14, pp. 4527-4530, 2011.
- [6] P. Seif, Johannes, A. Descoedres, M. Filipič, F. Smole, M. Topič, Z. C. Holman, S. De Wolf, C. Ballif, "Amorphous silicon oxide window layers for high-efficiency silicon heterojunction solar cells," *Journal of Applied Physics*, vol. 115, issue 2, p. 024502, 2014.
- [7] R. A. Street, *Hydrogenated Amorphous Silicon*. Cambridge, UK: Cambridge University Press, 1991.
- [8] V. M. Fthenakis, "Prevention and control of accidental releases of hazardous materials in PV facilities," *Progress in Photovoltaics*, vol. 6, issue 2, p. 91, 1998.
- [9] Silicon Valley Toxics Coalition, *Toward A Just And Sustainable Solar Energy Industry*. San Jose, USA, 2009.
- [10] E. Ore, G. Amaratunga, S. De Wolf, "HIT solar cell with V2Ox window layer," *MRS Advances*, vol. 2, issue 53, pp. 3147-3156, 2017.
- [11] E. Ore, J. Melskens, A. Smets, M. Zeman, G. Amaratunga, "MoOx hole collection layer for a-Si:H based photovoltaic cells," *MRS Advances*, vol. 1, issue 14, pp. 977-983, 2016.
- [12] E. Ore, G. Amaratunga, "Thin heterojunction a-Si:H photovoltaic cell design with no doped a-Si:H layers". In *40th IEEE Photovoltaic Specialist Conference (PVSC)*, 2014, pp. 3087-3089.
- [13] E. Ore, G. Amaratunga, "Cylindrical ultra-thin a-Si:H photovoltaic cell with no doped layers," *MRS Advances*, vol. 2, issue 15, pp. 825-833, 2017.
- [14] R. A. Sinton, "Development of an in-line minority-carrier lifetime monitoring tool for process control during fabrication of crystalline silicon solar cells," *Annual Subcontract Report for NREL National Renewable Energy Lab*, 2004.
- [15] M. J. Kerr, A. Cuevas, R. A. Sinton, "Generalized analysis of quasi-steady-state and transient decay open circuit voltage measurements," *Journal of Applied Physics*, vol. 91, issue 1, p. 399, 2002.